

Electronic Supplementary Information for: Substituent Effects on the Mechanochemical Response of Zinc Dialkyldithiophosphate

Jie Zhang, James P. Ewen* and Hugh A. Spikes*

Department of Mechanical Engineering, Imperial College London, South Kensington Campus, London SW7 2AZ, U.K.

* Corresponding author e-mails: j.ewen@imperial.ac.uk; h.spikes@imperial.ac.uk

Schematic of the ETM

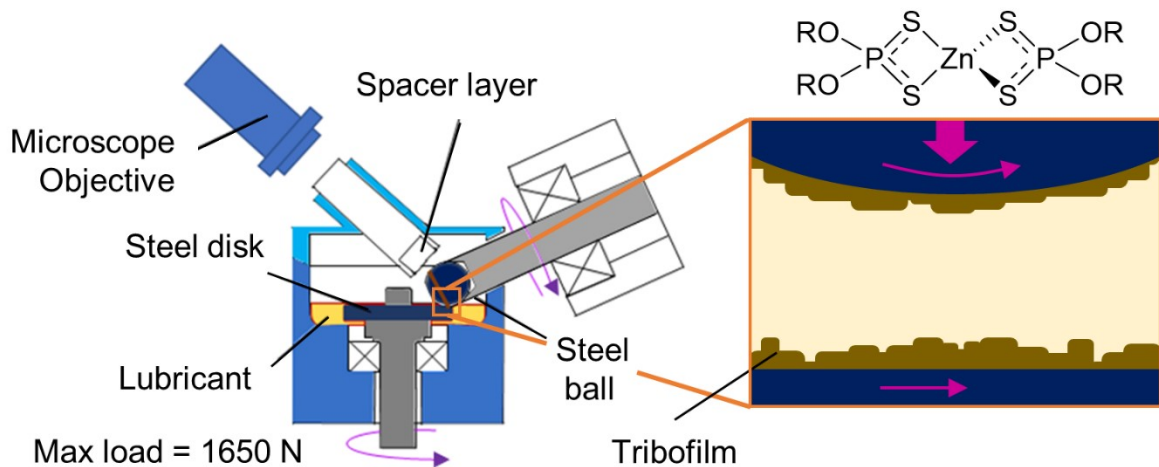
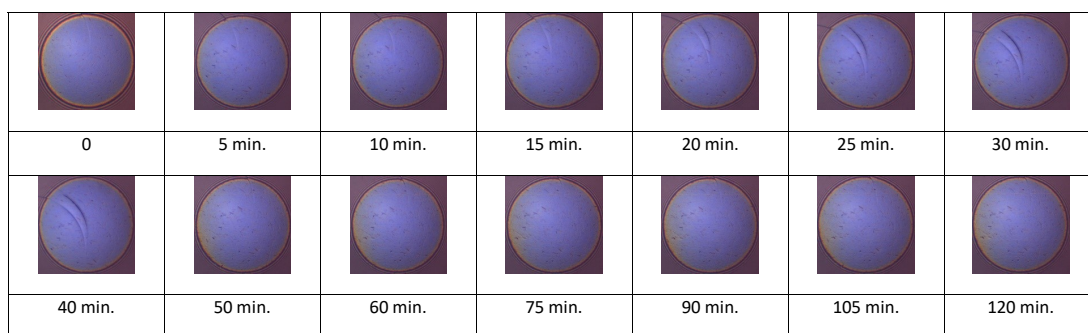


Figure S1. Schematic of the Extreme-pressure Traction Machine (ETM) tribometer and Spacer-Layer Imaging (SLIM) method used to monitor tribofilm thickness. In all the tribometer experiments, there is a fluid layer separating the steel surfaces. Adapted from Zhang et al.¹.

SLIM Images in PAO and Indopol H-8 (a)



(b)

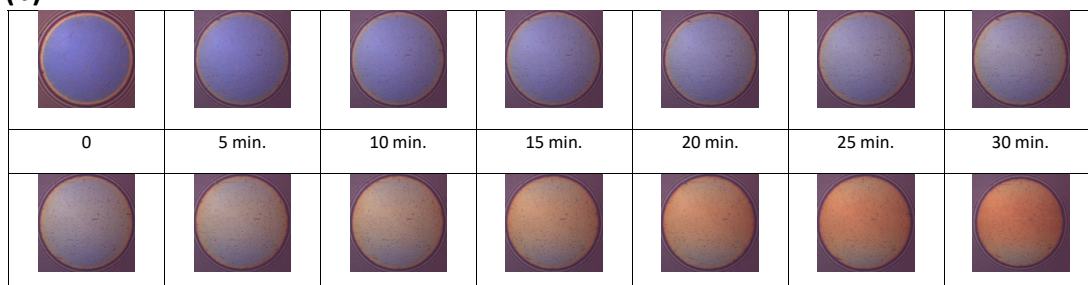


Figure S2. Comparison of SLIM images for oct-1-yl ZDDP in PAO10/PAO100 blend ($\mu = 0.04$) (a) and Indopol H-8 ($\mu = 0.09$) (b) at 80 °C and 1000 N.

Fluid Film Thickness

The measured film thickness values for Indopol H-8 have been corrected using the Chittenden equation² to allow for the difference in reduced elastic modulus, E' , and load, W , on EHL film thickness, via: $h \propto E'^{-0.12} W^{-0.073}$. For steel/steel contacts (AISI 52100), the reduced elastic modulus is 228 GPa,³ while for steel/glass it is 114 GPa. This results in the film thickness in the steel/steel contact being a factor of $(228/114)^{-0.12} = 0.92$ lower than for the steel/glass contact. Similarly, the fact that the maximum load used in the tribofilm growth experiments is 1500 N, while the film thickness measurements were made at 20 N, resulting in a film thickness reduction factor of $(1500/20)^{-0.073} = 0.73$. The values of h measured in the EHD2 have therefore been multiplied by $0.92 \times 0.73 = 0.67$ to obtain the estimated film thicknesses listed in Table S1.

Table S1. Measured EHL film thicknesses for Indopol H-8 at the entrainment velocity used in the tribofilm growth experiments ($U = 0.75 \text{ m s}^{-1}$) in a glass/steel contact at a load of 20 N. Corrected film thickness values are also shown to account for the higher reduced elastic modulus of a steel/steel contact and the larger maximum load ($W = 1500 \text{ N}$) used in the tribofilm growth experiments using the Chittenden equation. The λ ratio using the composite root-mean-square (RMS) roughness of the steel/steel contact (10.4 nm).

Temperature (°C)	Measured Film Thickness (nm)	Corrected Film Thickness (nm)	λ ratio
60	297	200	19
80	166	111	11
100	108	72	7
120	74	50	5

Table S2. Composite RMS roughness (R_{qc}) of tribofilms from the final SLIM images after 120 minutes of rubbing.⁴ Assuming equal roughness on ball (measured) and disk (assumed).

	Primary				Secondary		
	T (°C)	W (N)	R_{qc} (nm)		T (°C)	W (N)	R_{qc} (nm)
dodec-1-yl	80	1000	7.9	4-methylpent-2-yl	60	1000	4.7
	100	1000	12.1		80	1000	15.6
	120	1000	11.7		100	1000	4.2
	120	600	3.7		120	1000	45.7
	120	800	21.0		80	600	13.1
	120	1000	11.7		80	800	28.0
	120	1500	35.0		80	1000	15.6
oct-1-yl	60	1000	3.9	but-2-yl	80	1200	11.4
	80	1000	8.6		80	1500	41.9
	100	1000	11.5		60	1000	11.6
	120	1000	28.5		80	1000	3.7
	80	800	7.9		100	1000	15.4
	80	1000	8.6		120	1000	48.3
	80	1200	6.2		80	600	29.2
	80	1500	5.9		80	800	25.7
	120	600	5.4		80	1000	3.7
	120	800	7.2		80	1200	3.8
	120	1000	28.5		80	1500	25.1
	120	1500	34.9		60	1000	8.1
2- cyclohexylethyl	60	1000	3.7	oct-2-yl	80	1000	12.2
	80	1000	4.2		100	1000	35.0
	100	1000	9.3		120	1000	34.3
	120	1000	21.0		80	600	15.1
	80	800	6.0		80	800	18.5
	80	1000	4.2		80	1000	12.2

	80	1200	8.9		80	1200	6.0
	80	1500	17.4		80	1500	4.2
2-ethylhexyl	80	1000	3.8				
	100	1000	15.3				
	120	1000	11.4				
	80	800	8.3				
	80	1000	3.8				
	80	1200	7.5				
	80	1500	13.2				

EHL Friction Measurements

Table S3. Friction coefficients measured during the tribofilm growth experiments for the different ZDDPs under full-film EHL conditions.

	Primary				Secondary		
	T (°C)	W (N)	μ		T (°C)	W (N)	μ
dodec-1-yl	80	1000	0.097	4-methylpent-2-yl	60	1000	0.104
	100	1000	0.091		80	1000	0.098
	120	1000	0.084		100	1000	0.094
	120	600	0.083		120	1000	0.087
	120	800	0.085		80	600	0.102
	120	1000	0.084		80	800	0.100
	120	1500	0.082		80	1000	0.098
oct-1-yl	60	1000	0.102	but-2-yl	80	1200	0.098
	80	1000	0.097		80	1500	0.096
	100	1000	0.091		60	1000	0.104
	120	1000	0.086		80	1000	0.098
	80	800	0.100		100	1000	0.093
	80	1000	0.097		120	1000	0.087
	80	1200	0.098		80	600	0.101
	80	1500	0.094		80	800	0.100
	120	600	0.085		80	1000	0.098
	120	800	0.086		80	1200	0.098
	120	1000	0.086		80	1500	0.095
	120	1500	0.084	oct-2-yl	60	1000	0.104
2-cyclohexylethyl	60	1000	0.105		80	1000	0.097
	80	1000	0.098		100	1000	0.093
	100	1000	0.094		120	1000	0.087
	120	1000	0.089		80	600	0.100
	80	800	0.101		80	800	0.100

	80	1000	0.098		80	1000	0.097
	80	1200	0.099		80	1200	0.098
	80	1500	0.096		80	1500	0.095
2-ethylhexyl	80	1000	0.098				
	100	1000	0.093				
	120	1000	0.087				
	80	800	0.101				
	80	1000	0.098				
	80	1200	0.098				
	80	1500	0.095				

Table S4. Variation in mean and maximum Hertz pressure for steel/steel ball-on-disc (point) contact (19.05 mm ball diameter) for the load range considered in the tribofilm growth experiments.

Load (N)	Mean Hertz Pressure (GPa)	Maximum Hertz Pressure (GPa)
600	1.70	2.55
800	1.87	2.81
1000	2.01	3.02
1200	2.14	3.21
1500	2.31	3.47

Tribofilm Growth

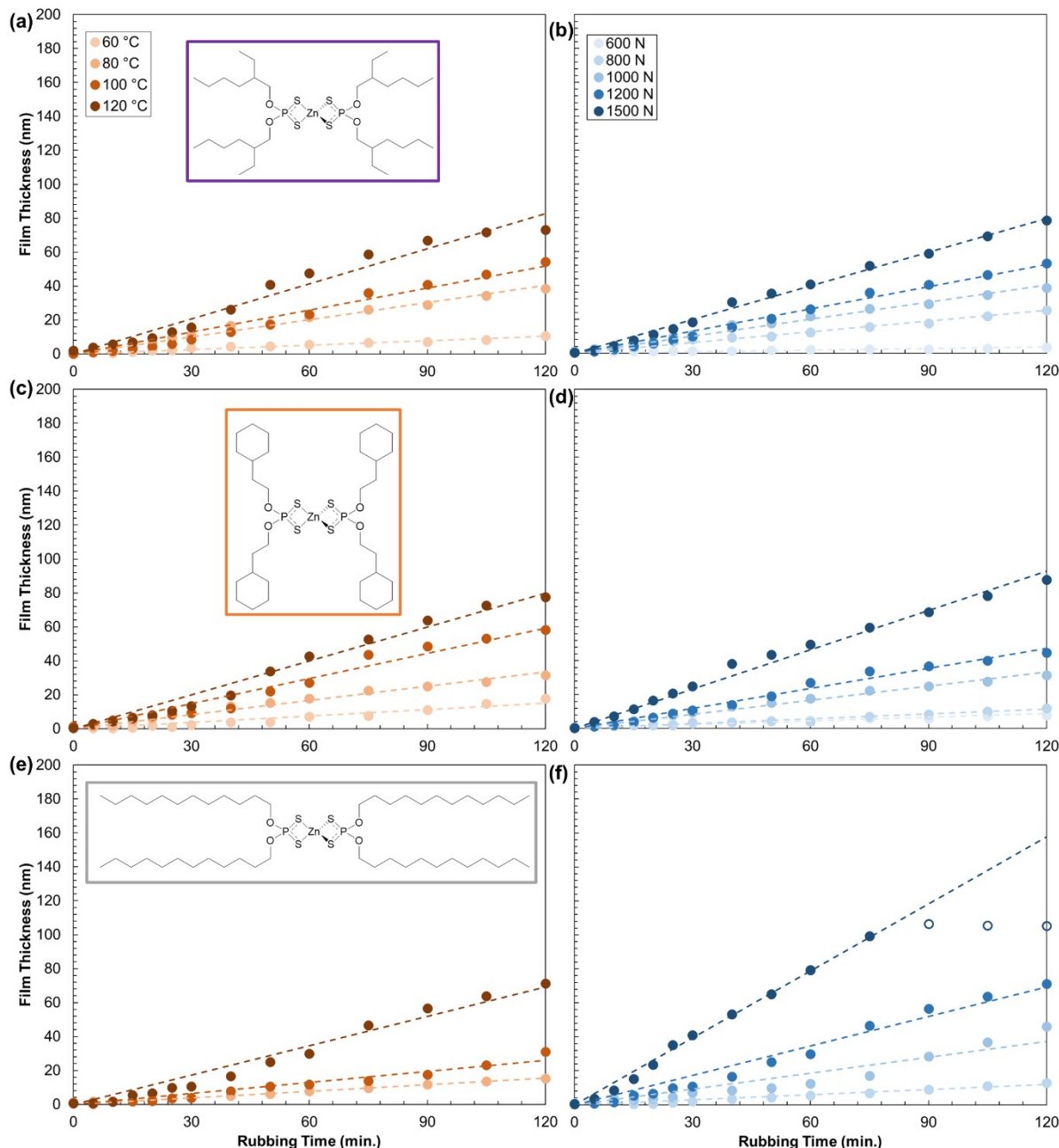


Figure S3. Variation in the tribofilm formation rate with temperature at a constant load of 1000 N (a, c, e) and shear stress at a constant temperature of 80 °C (b, d) or 120 °C (f) for primary 2-ethylhexyl (a, b), 2-cyclohexylethyl (c, d), and 1-dodecyl (e, f) ZDDPs. Dashed lines are the linear fits used to calculate the rates assuming zero-order kinetics; only the filled symbols are used for the fitting.

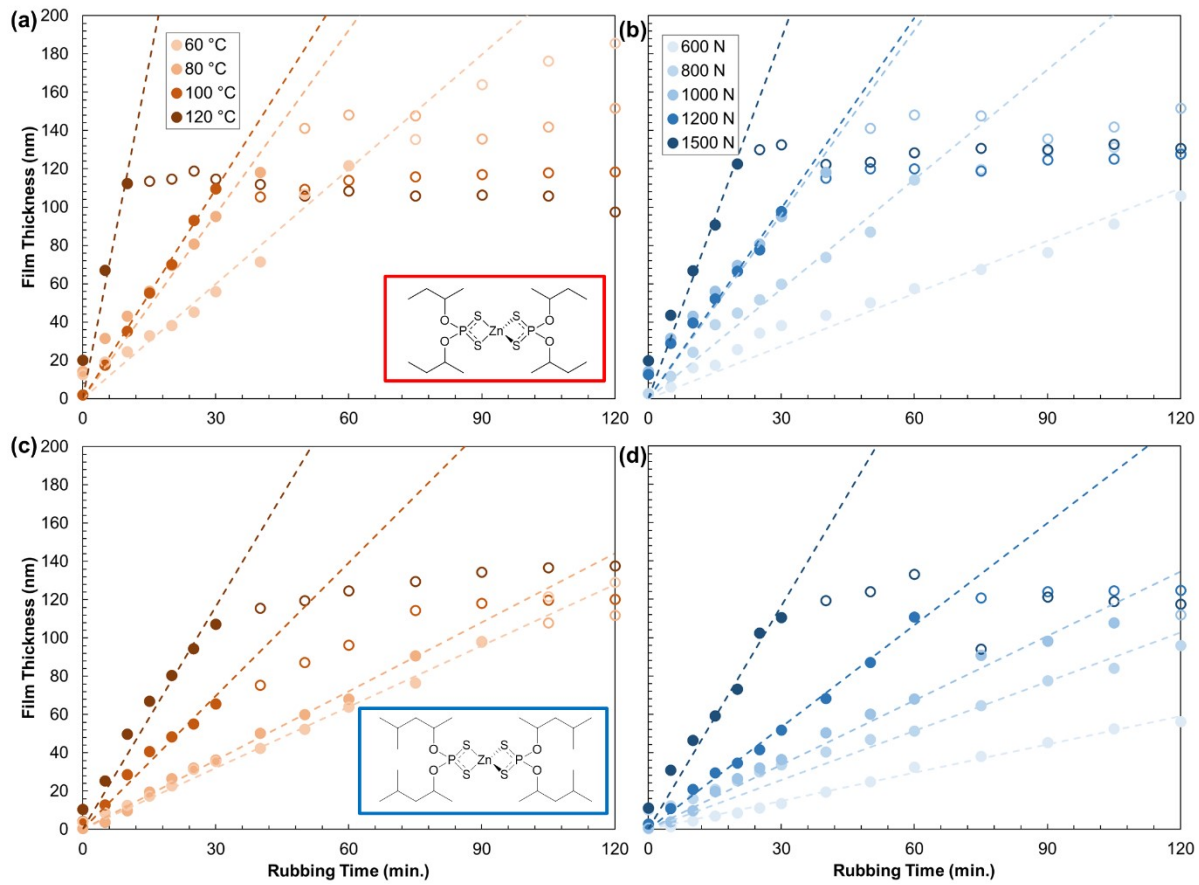


Figure S4. Variation in the tribofilm formation rate with temperature at a constant load of 1000 N (a, c) and shear stress at a constant temperature of 80 °C (b, d) for secondary but-2-yl (a, b) and but-2-yl (c, d) ZDDPs. Dashed lines are the linear fits used to calculate the rates assuming zero-order kinetics; only the filled symbols are used for the fitting.

Tribofilm Growth Rates

Table S5. Tribofilm growth rates used to produce Figure 5 obtained from linear fits in Figure 4 and Figure S4.

	Primary				Secondary		
	T (°C)	W (N)	Rate (nm min ⁻¹)		T (°C)	W (N)	Rate (nm min ⁻¹)
dodec-1-yl	80	1000	0.12	4-methylpent-2-yl	60	1000	1.07
	100	1000	0.24		80	1000	1.19
	120	1000	0.64		100	1000	1.53
	120	600	0.11		120	1000	2.78
	120	800	0.36		80	600	0.50
	120	1000	0.64		80	800	0.72
	120	1500	1.36		80	1000	1.07
oct-1-yl	60	1000	0.26	but-2-yl	60	1000	1.59
	80	1000	0.41		80	1000	2.31
	100	1000	0.66		100	1000	3.35
	120	1000	0.92		120	1000	9.22
	80	800	0.29		80	600	0.81
	80	1000	0.41		80	800	1.74
	80	1200	0.55		80	1000	2.31
	80	1500	0.65		80	1200	2.60
2-cyclohexylethyl	60	1000	0.14	oct-2-yl	80	1500	5.05
	80	1000	0.27		60	1000	0.62
	100	1000	0.52		80	1000	1.17
	120	1000	0.71		100	1000	1.70
	80	800	0.09		120	1000	3.40
	80	1000	0.27		80	600	0.65
	80	1200	0.40		80	800	0.65
2-ethylhexyl	80	1500	0.74				
2-ethylhexyl	80	1000	0.32				

	100	1000	0.48		80	1000	1.17
	120	1000	0.70		80	1200	1.86
	80	800	0.19		80	1500	2.41
	80	1000	0.32				
	80	1200	0.47				
	80	1500	0.68				

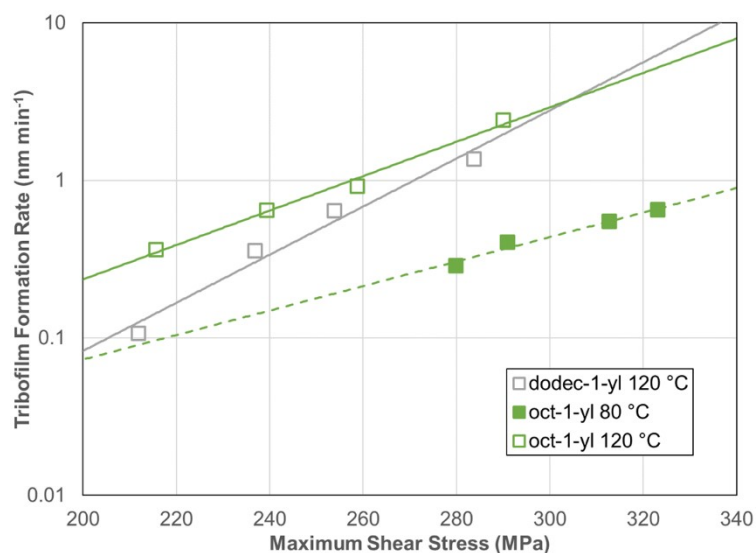


Figure S5. Change in the tribofilm growth rate for the dodec-1-yl and oct-1-yl ZDDPs with maximum shear stress, τ_{\max} , at 80 °C (filled squares) or 120 °C (open squares). Dashed lines are exponential fits of the data to the Bell model.⁵

Parameters for the Bell Model

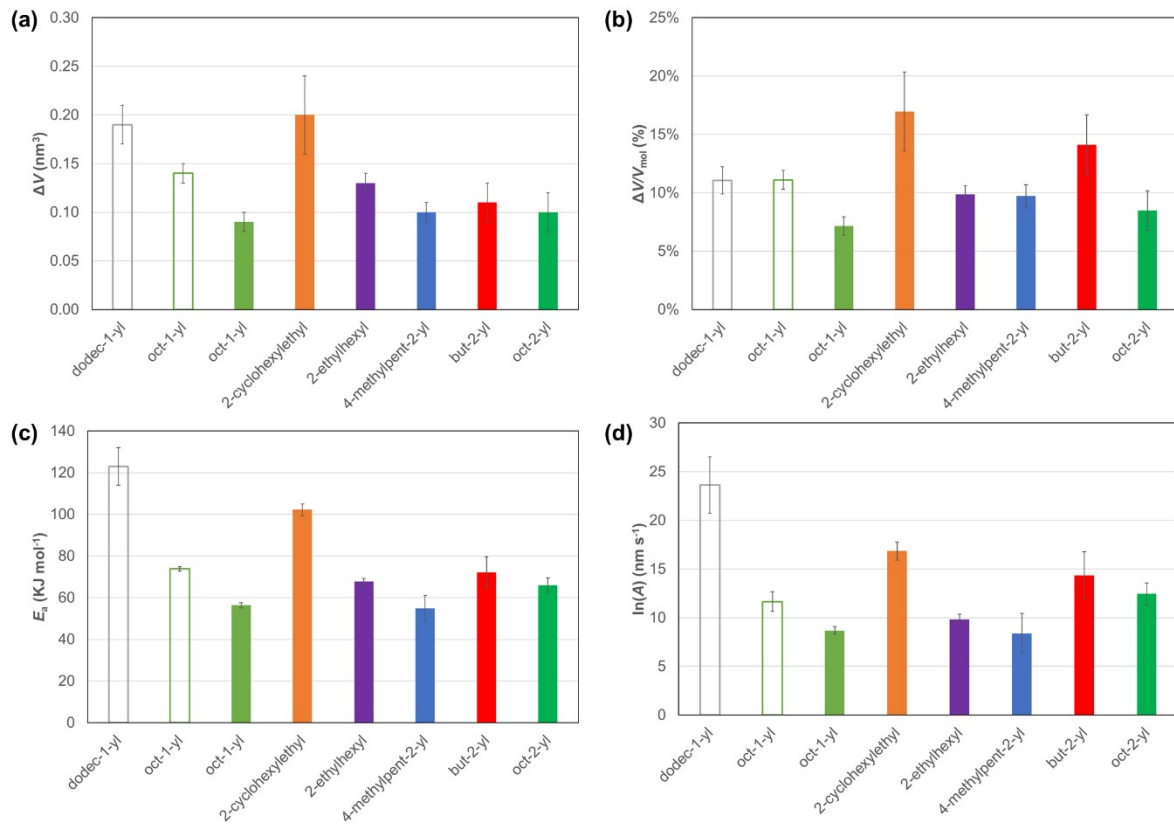


Figure S6. Kinetic parameters extracted from the fits to the Bell model⁵ shown in Figure 5. Vertical bars show 95 % confidence intervals. For filled bars, ΔV^* calculated at 80 °C and for open bars, ΔV^* calculated at 120 °C. E_a and A calculated at 1000 N.

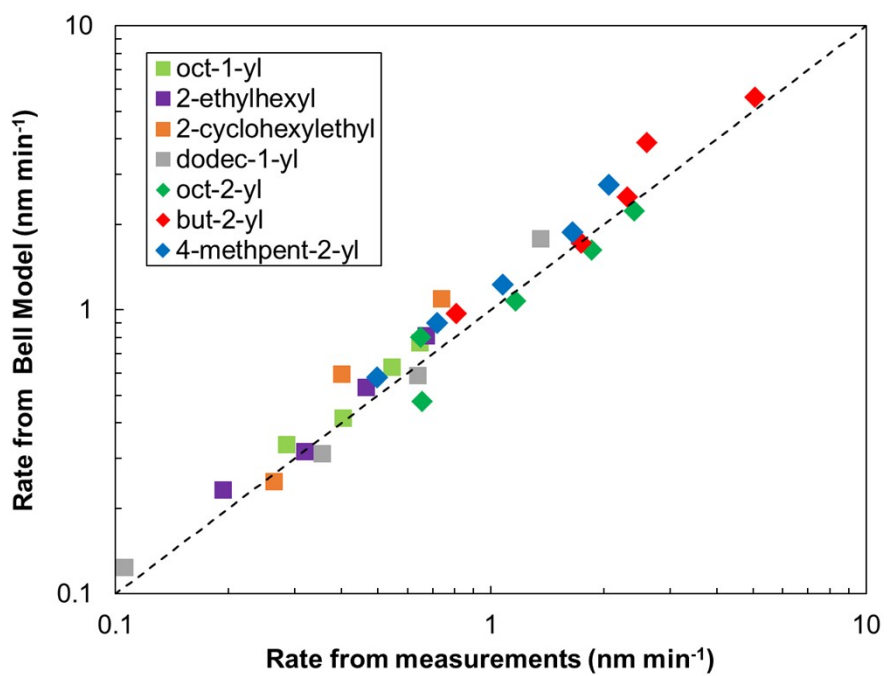


Figure S7. Comparison of measured rates with those predicted using the Bell model⁵, $R^2 = 0.9777$.

References

- 1 J. Zhang, J. P. Ewen, M. Ueda, J. S. S. Wong and H. A. Spikes, *ACS Applied Materials & Interfaces*, 2020, **12**, 6662–6676.
- 2 R. J. Chittenden, D. Dowson, J. F. Dunn and C. M. Taylor, *Proceedings of the Royal Society of London, Series A*, 1985, **397**, 245–269.
- 3 Y. B. Guo and C. R. Liu, *Journal of Manufacturing Science and Engineering*, 2002, **124**, 1–9.
- 4 K. Topolovec-Miklozic, T. R. Forbus and H. A. Spikes, *Tribology Letters*, 2007, **26**, 161–171.
- 5 G. I. Bell, *Science*., 1978, **200**, 618–627.